SEDIMENTOLOGY OF MODERN, INCLINED HETEROLITHIC STRATIFICATION (IHS) IN THE MACROTIDAL HAN RIVER DELTA, KOREA

KYUNG SIK CHOI,[1]* ROBERT W. DALRYMPLE,[1] SEUNG SOO CHUN,[2] AND SEONG-PIL KIM[3]
[1] *Department of Geological Sciences and Geological Engineering, Queen's University, Kingston, Ontario K7L 3N6, Canada*
[2] *Faculty of Earth Systems and Environmental Sciences, Chonnam National University, Gwangju, 500-757, Korea*
[3] *Petroleum and Marine Resources Division, Korea Institute of Geoscience and Mineral Resources, Daejeon 305-350, Korea*
email: tidalchoi@hotmail.com

ABSTRACT: **An occurrence of inclined heterolithic stratification (IHS) is described from a tidal point bar in a 40-m-deep distributary of the macrotidal (tidal range 3.6–7.8 m), Han River delta, Korea. The channel bank demonstrates a convex-upward profile with intermittent presence of wave-formed scarps and terraces near the low-water level. The vertical succession of IHS is approximately 25 m thick and dips into the channel with angles reaching 14°. The IHS overlies 15 m of trough cross-bedded sand deposited in the channel thalweg and lower point bar. Even though the channel as a whole is ebb dominated, the preserved cross bedding is predominantly flood directed because the mutually evasive nature of the ebb and flood currents causes the point-bar surface to be flood dominated. This pattern may be a common feature of tidal point bars. The IHS itself consists of interstratified fine sand, sandy silt, and silt with an upward-fining textural trend. Tidal rhythmites are well developed in the middle and upper intertidal zone, and may also be present in the subtidal zone, but are poorly developed near the low-water level because of wave action. Seasonal discharge variations of the Han River are not obvious in the deposits, because the large size, distal location, and energetic tidal environment of the studied channel reduces the impact of river-stage fluctuations. Despite the moderate salinity levels, bioturbation is rare, except in the upper intertidal zone, because of the rapid sedimentation and energetic conditions.**

INTRODUCTION

Inclined heterolithic stratification (IHS), previously known as epsilon cross stratification (Allen 1963) and longitudinal cross bedding (Reineck 1958), has received much attention in recent years. Although IHS may be produced by delta progradation (Stanley and Surdam 1978; Martinius et al. 2001), it is mainly formed by lateral accretion of point bars in meandering channels (Barwis 1978; Clifton 1983; De Mowbray 1983; Thomas et al. 1987; Smith 1988). Despite its presence in fluvial environments (e.g., Jackson 1981; Makaske and Nap 1995; Page et al. 2003), IHS appears to be particularly abundant in tide-influenced settings (Smith 1987, 1988; Thomas et al. 1987; Shanley et al. 1992; Kvale and Vondra 1993; Ainsworth and Walker 1994; Eberth 1996; Cotter and Driese 1998; Falcon-Lang 1998; Gingras et al. 1999; Gingras et al. 2002; Shanmugam et al. 2000; Martinius et al. 2001; Beets et al. 2003; Dalrymple et al. 2003). Indeed, there is a tendency to consider IHS to be a tidal indicator.

Despite the considerable number of reported occurrences in the ancient, relatively few studies have provided detailed descriptions of the vertical facies changes in IHS from modern tidal environments. Furthermore, available modern examples are mostly confined to small tidal creeks in microtidal and mesotidal settings, where the IHS is 1–4 m thick (Reineck 1958; Bridges and Leeder 1976; Barwis 1978; Clifton 1983; De Mowbray 1983; Smith 1988; Anima et al. 1989). No modern examples have been documented that are comparable to the very large (i.e., up to 25 m thick) examples of IHS reported from some ancient successions (e.g., the McMurray Formation—Mossop and Flach 1983; the Dunvegan Formation—Plint and Wadsworth 2003).

In this paper, we report a modern occurrence of large-scale (ca. 25 m thick) IHS from a distributary channel in the macrotidal Han River Delta, Kyonggi Bay, Korea. The sedimentary facies constituting the intertidal and subtidal portions of the IHS are described to derive a schematic stratigraphic model. Repeated echosounding and leveling surveys are used to document the morphodynamic change of the channel bank, in order to understand the origin and internal architecture of the deposits.

Study Area

Kyonggi Bay is the largest macrotidal embayment in Korea (Fig. 1) and contains an extensive system of tidal flats and NE–SW trending elongate tidal bars. The Han River, the largest river on the west coast of Korea, delivers sediment to Kyonggi Bay through four main distributary channels that are separated by bedrock islands. Sukmo Channel, lying between Kanghwa and Sukmo islands (Fig. 1B), is the most important distributary, with the highest tidal-current speeds and greatest depth. The channel averages 1000–1500 m wide and shows an S-shaped meander-like morphology, in which water is generally deeper on the outside of bends and shallower toward point bars (Figs. 1, 2). Locally, water depth reaches 50 m during spring high tides. Narrow, steeply dipping tidal flats are developed along both sides of the channel but are widest on the point bars. A tidal flat located 1 km west of Oepori Port and the adjacent subtidal portion of the channel were selected for this study (Fig. 1). A previous seismic survey conducted in this area showed that a progradational sediment body is developed near Kanghwa Island, with sediment thickness of nearly 50 m (KIER 1987).

Tidal ranges at Oepori Port are 7.8 m and 3.6 m during spring and neap tides, respectively. Maximum current speeds reach 2 m/s at the water surface, with an overall ebb dominance because of the river discharge (Chang and Oh 1991). Annual discharge of the Han River reaches 23 km^3/year, with nearly 60 percent of the discharge occurring in the three-month period from July to September (MCT 2001); the highest discharges occur in August. Water-level variations due to the change in river flow reach 1.5 m at Hangju Bridge (Fig. 3A) but are reduced to only 0.6 m at Oepori Port (KHO 2000). During the high-discharge period, the salinity is low but highly variable (9.6–18.7‰), with distinct stratification (Chang and Oh 1991). By comparison, the channel is partially to fully mixed during periods of low discharge, at which time the salinity is high and stable (25.6–28.5‰) (Chang and Oh 1991). Suspended-sediment concentrations also show large seasonal changes, ranging from $\sim$ 750 mg/l at times of low river discharge to $>$ 1500 mg/l during the rainy summer season (Chang and Oh 1991). Local mean wind is strongest ($>$ 2.5 m/s) and westerly in April, whereas the winds are weakest ($<$ 2.0 m/s) and northwesterly in October to December (KMA 2001, 2003; Fig. 3B).

METHODS

The subtidal morphology of the channel bank was determined using a single-channel NAVISOUND 215 echo sounder (Reson Co., Denmark)

* Present address: Petroleum and Marine Resources Division, Korea Institute of Geoscience and Mineral Resources, Daejeon 305-350, Korea

JOURNAL OF SEDIMENTARY RESEARCH, VOL. 74, NO. 5, SEPTEMBER, 2004, P. 677–689
 1527-1404/04/074-677/$03.00

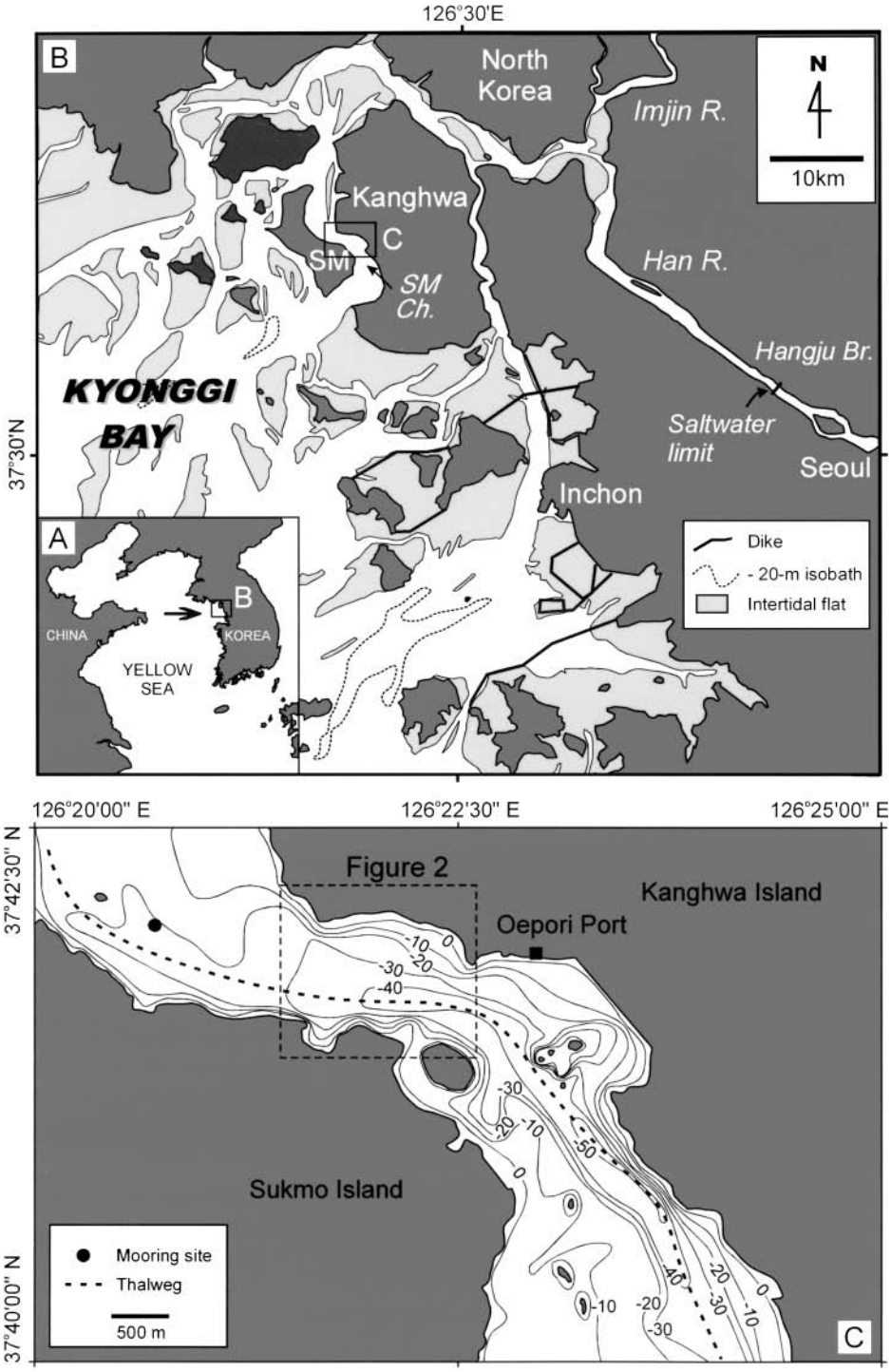

FIG. 1.—**A)** Map of Korean Peninsula showing location of Kyonggi Bay. **B)** Map of inner Kyonggi Bay showing study area in Sukmo Channel, the main distributary of the Han River. SM = Sukmo Island. **C)** Bathymetric map of Sukmo Channel in the vicinity of Oepori Port. Oceanographic data of Chang and Oh (1991) discussed in text obtained at current-mooring site (●).

with an operating frequency of 28–35 kHz. Positioning during the survey (Fig. 2) was accomplished using a differential GPS system with a horizontal accuracy of ± 1 m. Profiling of the intertidal portion of the channel bank was performed six times over a three-year period (March 2000; January and December 2001; and August, November, and December 2002) using a Dumpy Level (model: PS-1, Sokkia Co., Japan). Visual observations without leveling were made at four additional times (November 1999; May and June 2000; and June 2001). A natural outcrop 6 m high and 40 m long, which was formed by unusually high discharge from a transverse runoff channel, permitted detailed examination of the intertidal facies.

Sediment samples were collected from the intertidal portion of the bank using can cores; a grab sampler was used in the subtidal area. Two vibracores (3–4 m long) were also obtained from the lower and middle portions of the intertidal area (Fig. 2). The grain size of the sediment was determined using the conventional sieving technique for the sand fraction and a Sedigraph 5100D for the silt and clay fractions. For the detailed analysis of physical lamination, selected samples were impregnated using

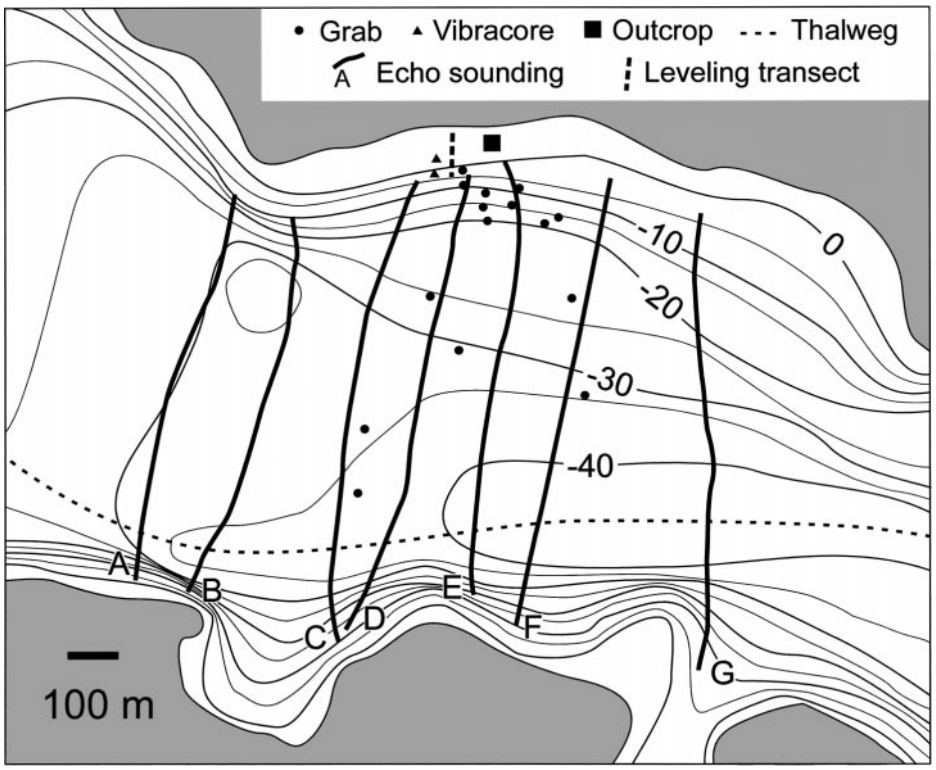

FIG. 2.—Bathymetric map of study area showing locations of echo-sounding lines, grab samples, outcrop, and leveling transect. Contour interval is 5 m. See Figure 1C for location.

low-viscosity Spurr Resin and thin-sectioned. The upper 5–10 cm of undisturbed grab samples from the subtidal zone was also logged for sedimentary structures.

RESULTS

Channel and Channel-Bank Morphology

Sukmo Channel is narrowest and most sinuous in the vicinity of the study site (Fig. 2). Echo-sounder profiles show that the channel is relatively flat floored (Fig. 4). Reflector character indicates that most of the channel bottom is sediment covered. Most of small-scale irregularities on the channel floor are dunes except near the downstream end of study area, where bedrock outcrops become abundant (Fig. 4). In contrast to the steeply inclined (10–25°) channel margin near Sukmo Island (cutbank), the subtidal bank near Kangwha Island (point bar) is relatively gentle with the mean inclination varying between 3 and 14° (Fig. 4). In places, the point-bar surface shows a step-like morphology with a terrace at a depth of approximately 20–30 m below mean sea level (Fig. 4C, G).

The width of the intertidal portion of the channel bank, as exposed at spring low tide, ranges between 50 and 80 m. This area has a convex-up profile, with typical slopes of 11–12° in the lower intertidal zone, 7–8° in the middle intertidal zone, and 0–2° in the upper intertidal zone (Figs. 5, 6). When sedimentation is active, the convex-up profile is smooth. More commonly, however, the profile is broken by one or more small (5–10 cm high), erosional scarps (Fig. 7A). More prominent scarps up to 1 m high, fronted by terraces 5–10 m wide, are intermittently developed in the lower intertidal zone, below mean sea level (Figs. 6 and 8A).

Repeated profiling of the intertidal area reveals that the channel bank prograded significantly during the first two years of monitoring, after which time there was relative stability, with the development of prominent erosional scarps (Fig. 6). The most pronounced changes occurred in the lower intertidal zone, where the channel bank prograded more than 15 m over 21 months (between March 2000 and December 2001), retreated about 8 m over three months with the development of prominent scarps (between August and November 2002), and then retreated another 6 m in just one month (between November and December 2002). The magnitude of the changes decreases toward the high-tide level, with the upper intertidal zone exhibiting only a small amount of aggradation. These observations indicate that the channel bank alternates between depositional and erosional phases with no apparent periodicity. During each erosional episode, exposure of older stratification is common (Fig. 7A), and eroded blocks of sediment may be present at the bases of the scarps (Figs. 7B, 8A). During the subsequent depositional phase, the eroded portion of the channel bank becomes a locus of rapid sedimentation, which eventually buries the scarp and returns the bank to a smooth, convex-upward profile (Fig. 8B). The newly deposited sediment is easily distinguishable from older material because the former is watery and soft, whereas the latter is stiff and compact.

Surface-Sediment Distribution and Sedimentary Facies

Subtidal grab samples demonstrate that the surface sediment of the channel bank exhibits an upward-fining trend: the channel-bottom area (i.e., deeper than 35 m) is covered by gravel and coarse sand; the lower portion of the bank (20–35 m depth) consists of medium sand; and the subtidal area shallower than 20 m consists of fine sand to sandy silt. The intertidal portion of the channel bank continues the upward fining, with sandy silt (mean grain size: 5–5.3 phi; 25–31 μm) in the lower intertidal zone passing upward to fine silt (mean grain size: 6–6.6 phi; 10–16 μm) in the upper intertidal zone near the high-tide elevation. The only departure from this trend occurs in the area at and just below the mean low-water level (ca. -5 m), where grain sizes are slightly coarser than above and below this elevation.

On the basis of the echograms, large ebb-oriented dunes up to 3 m in height and 100 m in wavelength are formed on the channel floor near Sukmo Island (cutbank) side in water depths between 20 and 40 m. By contrast, on the Kanghwa Island (point bar) side, flood-oriented dunes of the same size occur in water depths between 20 and 35 m. Dunes are not present in the shallow subtidal zone (above the -20 m level) on the point-

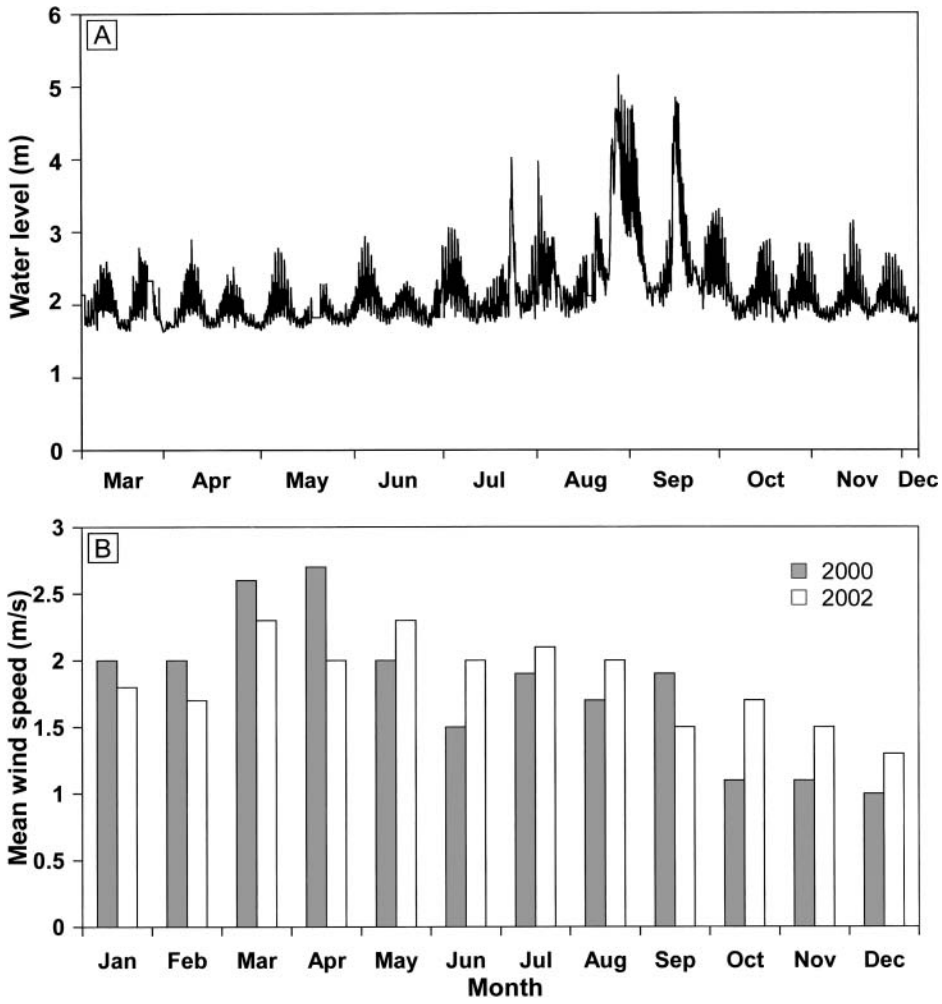

FIG. 3.—**A)** Water-level data at Hangju Bridge (See Figure 1B for location), Han River (MCT 2001). Because of the presence of a weir at this location, true low-tide water levels are not recorded and the full tidal range is not shown. Note the prominent discharge peaks in the July to September period. **B)** Seasonal variation of average wind speed, Oepori Port (KMA 2001, 2003). The strongest winds are generally in the March to May period.

bar surface, although they do occur at such elevations on the cutbank side of the channel. Current ripples may be present in the shallow subtidal area, but they are present only locally in the intertidal zone, where their crestlines show a migration direction parallel to the channel.

The degree of bioturbation varies with elevation from low in the subtidal and lower intertidal zones to high in the upper intertidal zone. The burrows are produced primarily by small crabs (e.g., *Ilyoplax pusilla*) (Fig. 7C). Mud pebbles eroded from preexisting channel-bank deposits are scattered on the terrace downslope from each erosional scarp (Fig. 7B). Rill marks are typically developed below mean sea level and are deepest and most extensive near the mean low-tide level (Fig. 7D), where the slope is steepest. Salt-marsh plants are present in the upper intertidal zone, which is submerged only during perigean spring tides. Polygonal mud cracks are also characteristic of this zone (Fig. 7E), leading to blocky erosion. The walls of the mud cracks and burrows in the upper intertidal zone are typically oxidized and coated with iron hydroxide. Shell fragments are not found in the intertidal or subtidal portions of the channel bank.

Because of the vertical changes in grain sizes and bedforms described above, the facies constituting the Sukmo Channel bank vary with elevation. The deposits of the deeper part ($>$ 20 m) of the channel will consist of cross-bedded medium to coarse sand, resting on a gravel lag that marks the channel base. Bedform facing directions in the echograms indicate that the paleoflow direction recorded by the cross bedding will be bipolar: flood orientations will predominate, but ebb orientations may be present in the deposits formed in the channel thalweg. Any mud drapes that may have been deposited on the dunes during slack water were not detected in the grab samples, so they are either volumetrically small or are not preserved.

Examination of the undisturbed grab samples shows that the succession above these cross-bedded sands (i.e., areas above -20 m) is dominated by interstratified sand and mud. At water depths of approximately -20 to -18 m, a laminated sand facies consisting of alternating medium sand and mud is found. The local presence of small dunes, as seen on echograms, indicates that the sand layers may be cross bedded. The mud layers are up to 1 cm thick and overlie the sand without gradation. Between approximately -18 m and the neap low-water level in the intertidal zone, the deposits consist of interstratified fine to very fine sand and mud. In contrast to the sharp contacts that occur in the underlying, laminated sand facies, each sand and overlying mud lamina constitute a normally graded couplet (Fig. 9A, B) that is typically less than 5 mm thick. The thicker sand layers are commonly ripple cross-laminated. Flame structures are common, and bioturbation is rare to absent.

A laminated silt facies is present at elevations between the neap low-water level and neap high-water level (Fig. 9C, D); the laminae in this facies consist of coarse to fine silt and have thicknesses that are less than 5 mm. Ripple cross lamination is locally present with set thicknesses less than 3 cm. Bioturbation is rare but gradually becomes more prevalent with increasing elevation. Laminae are traceable laterally for as much as 100 m along the strike of the channel bank, but their extent in the dip direction is broken by the erosion surfaces associated with the scarps. Lamina thickness shows various tidal rhythmicities, ranging from daily to monthly (see

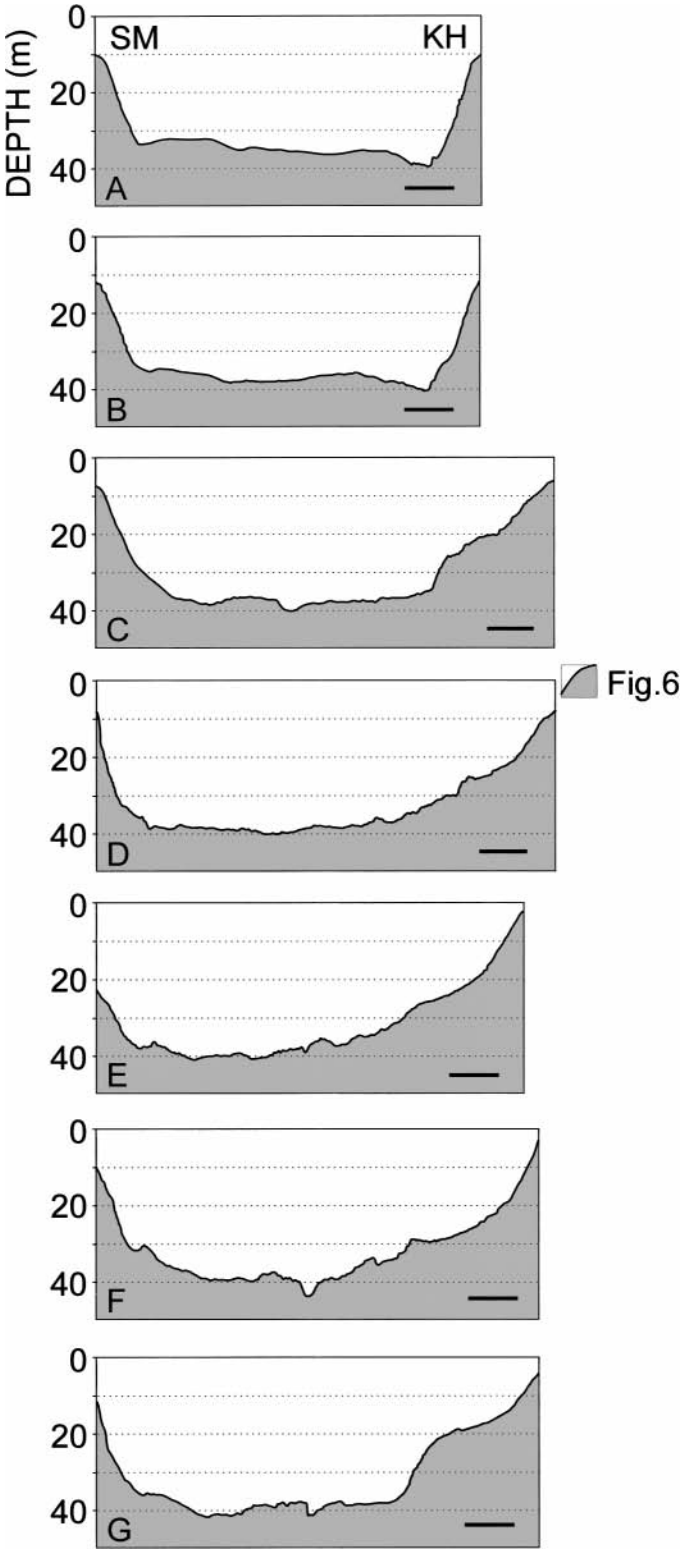

FIG. 4.—Cross-sectional profiles of Sukmo Channel, drawn from echo-sounding and leveling records. See Figure 2 for location of sections. Horizontal scale bars are 100 m; vertical exaggeration is ca. 8.2 times. Depths are below mean sea level. SM and KH denote Sukmo Island and Kanghwa Island, respectively.

below). Convolute lamination is moderately common, with deformed intervals reaching up to 20 cm thick (Fig. 10). Both symmetric and plunging asymmetric folds are present; the anticlinal folds are commonly overturned in the downslope direction (Fig. 10). Each deformed interval is usually truncated by an erosion surface linked to a scarp and overlain by planar lamination (Fig 10C). This deformation may be triggered by waves, accompanied by gravity-driven downslope movement. The presence of tensional cracks in the upper intertidal zone supports this interpretation. Similar convolution structures have been observed in other tidal-channel banks (Barwis 1978; Allen 1985; Anima et al. 1989; Larsonneur 1994).

The deposits above the mean neap high-water level are dominantly laminated mud (fine silt to clay), in which lamina thickness rarely exceeds 1 mm (Fig. 9E, F). Tidal rhythmicities are not as well developed as in the coarser deposits at lower elevations. Microscale ($<$ 1 cm relief) flame structures are common, and bioturbation is moderate to intense. Fine rootlets and disseminated plant debris, which are remnants of salt-marsh plants that grow during the spring and summer, are common in these laminae.

Tidal Rhythmicities

Three kinds of tidal rhythmicities are recognizable in plots of the variation of laminae thickness, occurring mainly within the laminated silt facies that forms just above mean sea level (between 1 and 2 m). (1) The alternation of individual thick and thin laminae (Fig. 11A, B) is interpreted to represent a diurnal cycle caused by the diurnal inequality of the semidiurnal tides: the thick laminae were deposited during the larger tide and the thin laminae by the smaller tide. (2) Quasi-sinusoidal variations of lamina thickness in groups of less than 30 laminae (Fig. 12) are interpreted to represent the neap–spring (synodic) cycle, which has a length of 28 tidal cycles. In these cycles, thicker and siltier laminae indicate spring tides, and thinner and muddier ones represent neap tides. Many of the neap–spring cycles are incomplete, however, and contain less than 28 laminae, either because of nondeposition during neap tides or erosion during spring tides. Asymmetric cycles, in which the laminae thin progressively upward from an abrupt base, are also common. This pattern may reflect nondeposition or erosion as the tidal-current speeds increase from neap to spring tides, followed by deposition as the current wanes from spring to neap tide. Microscale load and flame structures are present where muddy laminae representing neap tides are abruptly overlain by thicker sandy laminae presumably formed during spring tides (Fig. 13). Such flame structures are preferentially overturned toward the channel. (3) In some intervals, a third type of cyclicity is observed in which thicker and coarser-grained neap–spring cycles alternate with thinner cycles that are finer grained (Figs. 11C, 12). This rhythmicity represents the anomalistic tidal cycle, in which the thicker neap–spring bundle represents perigean spring tides (high springs), while the thinner one was deposited during apogean spring tides (low springs) (Kvale et al. 1999).

The thickness of the neap–spring cycles decreases with increasing elevation (Fig. 13), from 1–3 cm near mean sea level to less than 0.5 cm near mean high-water level. Similarly, the number of preserved laminae in each cycle decreases from 8–30 near mean sea level to 5–15 near mean high-water level. As a result, tidal rhythmicity becomes more incomplete toward higher elevations, a feature that presumably is related to the smaller number of submergence events (e.g., Dalrymple et al. 1991; Tessier 1993; Choi et al. 2001). The increased degree of bioturbation also contributes to the poorer preservation of tidal rhythmicity at higher elevations. Sediments below mean sea level also show progressive deterioration of the tidal rhythmicity, despite the notable increase of layer thickness (up to 5 cm) in response to more rapid sedimentation closer to the channel. We attribute this to the unconsolidated and watery nature of the sediments as a result of shorter emergence times, which makes these deposits less resistant to erosion by even small waves (cf. Lawler et al. 2001).

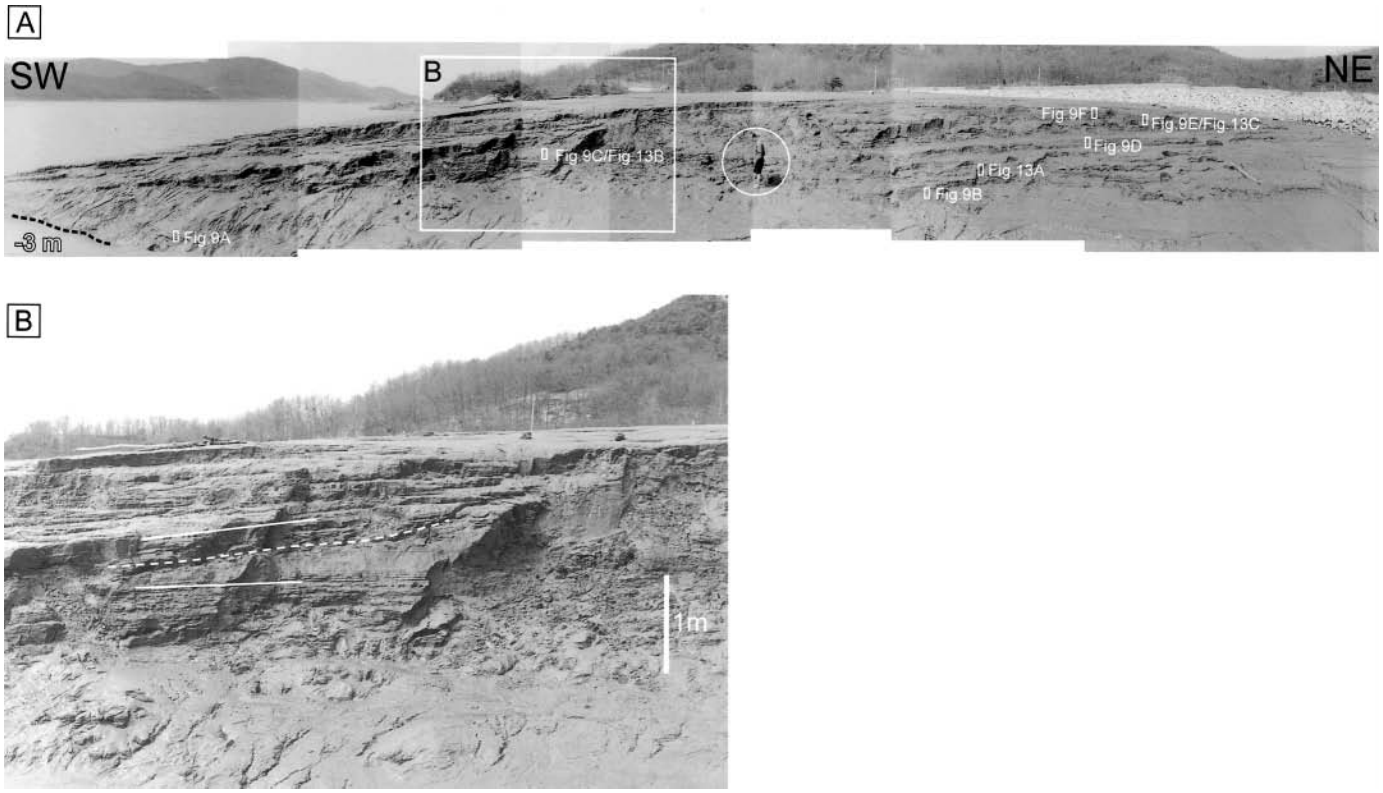

FIG. 5.—**A)** Photomosaic showing outcrop section of Sukmo Channel bank at the study site. Locations of can-core samples are shown. Note person (circled) for scale. Refer to Figure 2 for location of the section. **B)** Enlarged view of the exposed section illustrating convex-up erosion surface (dashed line). Overlying strata onlap this surface and dip more steeply than the underlying strata.

DISCUSSION

Rapid Sedimentation and Preservation Potential

The studied portion of the Sukmo Channel bank prograded and aggraded significantly over the 33-month study period (Fig. 6). The average sedimentation rate as calculated from the elevation differences between the initial and final profiles decreases with elevation, from about 8 cm per month in the lower intertidal zone near the mean low-water level, to about 3 cm per month in the upper intertidal zone near the mean high-water level. The latter value is compatible with that deduced from the tidal rhythmites. On the basis of the neap–spring tidal cyclicity, the sedimentation rate decreases with elevation from 5 cm per month near the mean neap high-water level, to less than 1 cm per month near the mean high-water level. By contrast, comparison of the sedimentation rates determined by profiling and analysis of tidal rhythmites is not straightforward for the lower intertidal portion of the bank, where tidal rhythmicity is not well defined in the deposits: the maximum sedimentation rate obtained from profiling is 40 cm per month, whereas the deposits suggest that the sedimentation rate may reach 5 cm per tidal cycle (assuming that a single graded layer (e.g., Fig. 9A) is formed in one tidal cycle). If such a high sedimentation rate were to persist, then theoretically as much as 2 m of sediment might accumulate in one month. However, sedimentation rates of this magnitude are not maintained for long, because of the unconsolidated nature of sediment and the frequent occurrence of wave erosion on the lower intertidal portion of the bank.

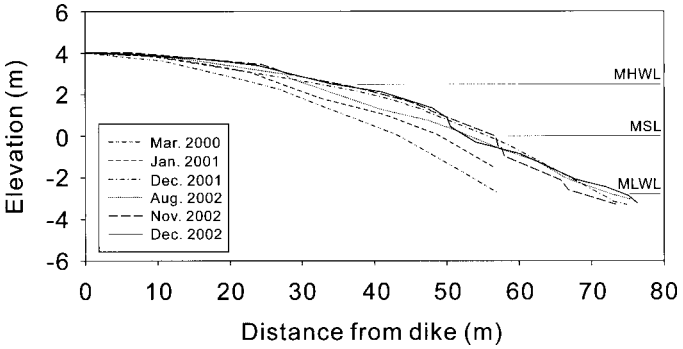

FIG. 6.—Repeated profiles of Oepori channel bank. Note alternation of progradation/aggradation and retreat over short time intervals, especially in the area below mean sea level (MSL). Prominent erosional scarps existed in November and December 2002. MHWL, mean high-water level; MLWL, mean low-water level.

Environmental conditions within Sukmo Channel show distinct seasonality, with river discharge and suspended-sediment concentration being greater during the wet summer months (Fig. 3A). Despite these changes, there is little obvious sedimentary record of this seasonal variation. Following Kvale et al. (1994), it could be suggested that some of the thicker neap–spring bundles that occur near mean sea level (Figs. 11, 12) formed during the time of increased river discharge. However, sedimentation rates of the magnitude indicated by these rhythmites occurred during all seasons (Fig. 6); therefore, such a seasonal interpretation cannot be assumed. The episodic occurrence of erosional events also breaks the continuity of the rhythmite successions, such that the length of the longest continuous record is too short to show seasonal variations in lamina thickness. Consequently, the paucity of evidence of seasonal sedimentation is a direct result of the high-energy conditions and rapid sedimentation that characterize the channel throughout the entire year. Furthermore, the change in water level caused by the increased discharge (< 0.6 m) is very small compared to

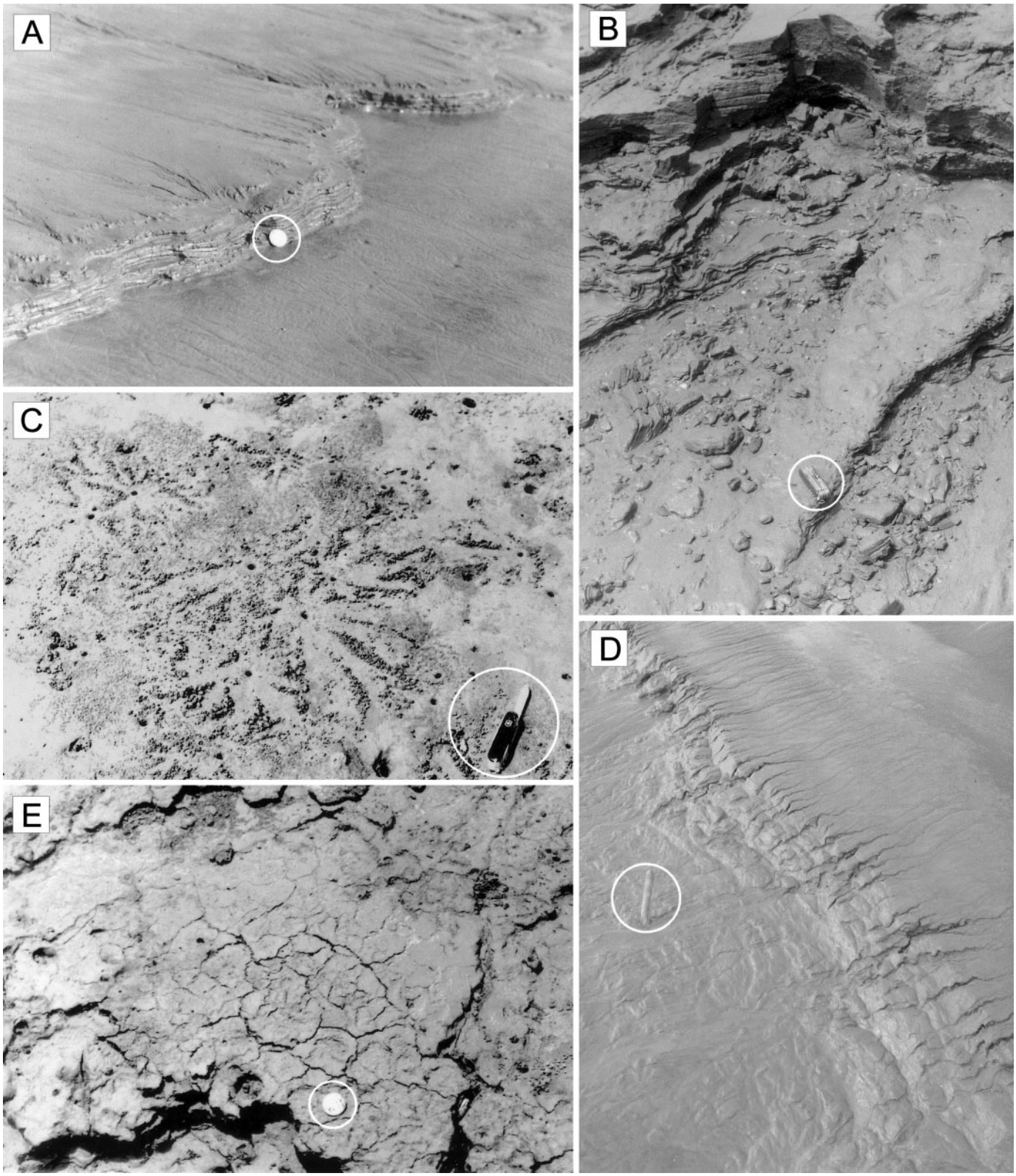

FIG. 7.—Photographs showing surface features of the intertidal zone. **A)** Erosional scarp exposing interlaminated mud and very fine sand to silt (elevation 0.8 m above mean sea level). Newly deposited sediment occurs below scarp, which is in the process of being healed. Coin is 2.5 cm in diameter. **B)** Mud pebbles at base of actively retreating erosional scarp, lower intertidal zone (−1.5 m). Knife is 9 cm long. **C)** Small crab burrows in the upper intertidal zone (+2.1 m). Knife is 14 cm long. **D)** Bifurcating rill marks (+1.1 m) at the site of an erosional scarp that is being buried by new deposits. Spatula handle is 10 cm long. **E)** Polygonal mud cracks in the upper intertidal zone (+2.5 m). Coin is 2.5 cm in diameter.

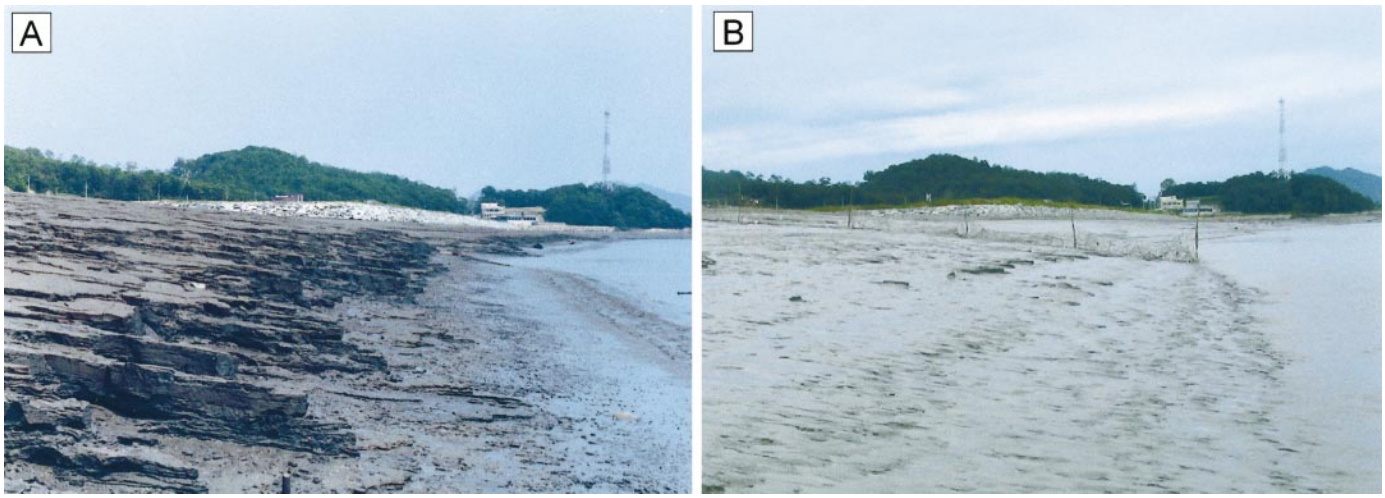

FIG. 8.—Photographs showing changes in channel-bank morphology. **A)** Erosional phase with prominent scarp approximately 1 m high (May 24, 2000). **B)** Depositional phase with previous scarp nearly completely buried by soft mud forming a smooth, convex-up surface (29 August 2002).

the tidal range (5–9 m) in the study area. Because of this, the seasonal changes may have only subtle affects on sedimentation.

Origin of Terraces

Repeated profiling and visual observations show that the upper part of the channel bank undergoes an apparently nonperiodic alternation of erosional and depositional intervals (Figs. 6, 8, 14). Formation of the scarps is believed to be caused by erosion by waves (cf. Lawler et al. 2001), despite the sheltered location of the study site (Fig. 1). Field observations and climate data (KMA 2001, 2003) indicate that the channel bank retains its convex-up morphology during calm-weather conditions, whereas erosional scarps occur during periods when westerly winds exceeded a daily-average speed of 2.5 m/s and locally generated waves are more than about 30 cm high. For instance, late March and April 2000 were very windy months when average and maximum wind speeds were 2.5 m/s and 10 m/s, respectively. These conditions are thought to be responsible for the scarp shown in Figure 8A. The erosional scarps of November and December 2002 may have been initiated by two very windy days (October 19, 20) when daily-average wind speed was over 4 m/s. It appears that lower winds and smaller waves are capable of maintaining the scarps, once they are initiated, only a relatively prolonged period of calm weather (of the order of 2–3 months) allows sedimentation to heal the erosion scar. Winds from the west-northwest are most likely to cause erosion because this is the direction of maximum fetch along the length of the channel (Fig. 1). The lower intertidal zone is most prone to erosion: these sediments are less cohesive than sediments at higher elevations because they are exposed for a shorter time and experience less desiccation-related consolidation.

Echo sounding reveals that the subtidal portion of the channel bank also possesses a terraced morphology (Fig. 4), but at a depth that is too deep for wave action to be important. It is possible that the terraces, which are larger than those in the intertidal zone, could be bedrock-cored features, but no bedrock outcrops were recognized on the echo-sounder records. Therefore, it appears that the terraces are of sedimentary origin. Tidal currents might form terraces either by direct scour at the level of the terrace or by local impingement of the thalweg against the channel bank, with scour to the channel floor, followed by vertical aggradation of the terrace after the channel thalweg moved away from the bank, in the manner observed in the Cobequid Bay–Salmon River estuary (Zaitlin 1987; Dalrymple and Zaitlin 1994). The fact that the terraces occur near the mid-channel depth, where current speeds during both the flood and ebb are not likely to be strong, suggests that they are not current-produced erosion features. This is supported by the fact that the terraced morphology is least well developed in the location where the currents are likely to be strongest (i.e., at the bedrock headlands that lie immediately to the east and west of the study area (Fig. 1B). Bank erosion by meanders of the channel thalweg, followed by vertical aggradation, is also unlikely because there is no evidence in the bathymetric data to suggest that the thalweg has the tight sinuosity required to create the concave indentations in the channel bank (Fig. 2). The mechanism of flow separation advanced by Bridges and Leeder (1976) and De Mowbray (1983) to explain terraces in tightly meandering intertidal creeks can also be discounted here because the terraces occur far below the low-tide level.

Instead, we suggest that the terraces may be the result of large-scale failures of the upper part of the point bar. The channelward dip of the interbedded sand and mud strata create the ideal situation for slumping, as indicated by the prevalence of convolute bedding and tensional fractures in the intertidal portion of the bank. The rapid rate of progradation of the intertidal portion of the bank (Fig. 6) also creates the potential for bank instability. In addition, bank accretion would progressively constrict flow within the channel, perhaps leading to scour and undercutting of the toe of the slope. The concave-northward shape of the −10 and −20 m contours at the location of profiles D to F (Fig. 2) may represent the site of a former large-scale failure, with the broad terrace between −20 and −30 m being the slump debris. It is perhaps significant that the terrace lies at the lowest elevation at which interbedded sand and mud occur, with failure having occurred on the upper part of the slope, where many potential failure planes exist.

Stratigraphy and Architecture

A schematic columnar section of the channel bank is provided in Figure 15. The deep subtidal portion (> 20 m) of the succession is inferred from echograms and grab samples to consist of trough cross-bedded sand facies. The orientation of the cross bedding is likely to be parallel to the channel margin, with a flood dominance, as indicated by the echo-sounder data. Thick slump deposits derived from failure of the heterolithic upper part of the succession may also be present (Fig. 15), if the suggested origin of the bank concavity near the intertidal leveling transect (Fig. 2) is valid.

The upper 20–25 m of the succession is dominated by IHS (Fig. 15). The inclination of the stratification ranges between 1° and 14°, with a marked upward decrease in the dip. Lamina/bed thickness also decreases upward, and there is an overall upward-fining trend, from medium sand at the base, to fine silt and clay at the high-tide level. Bioturbation is greatest in the upper

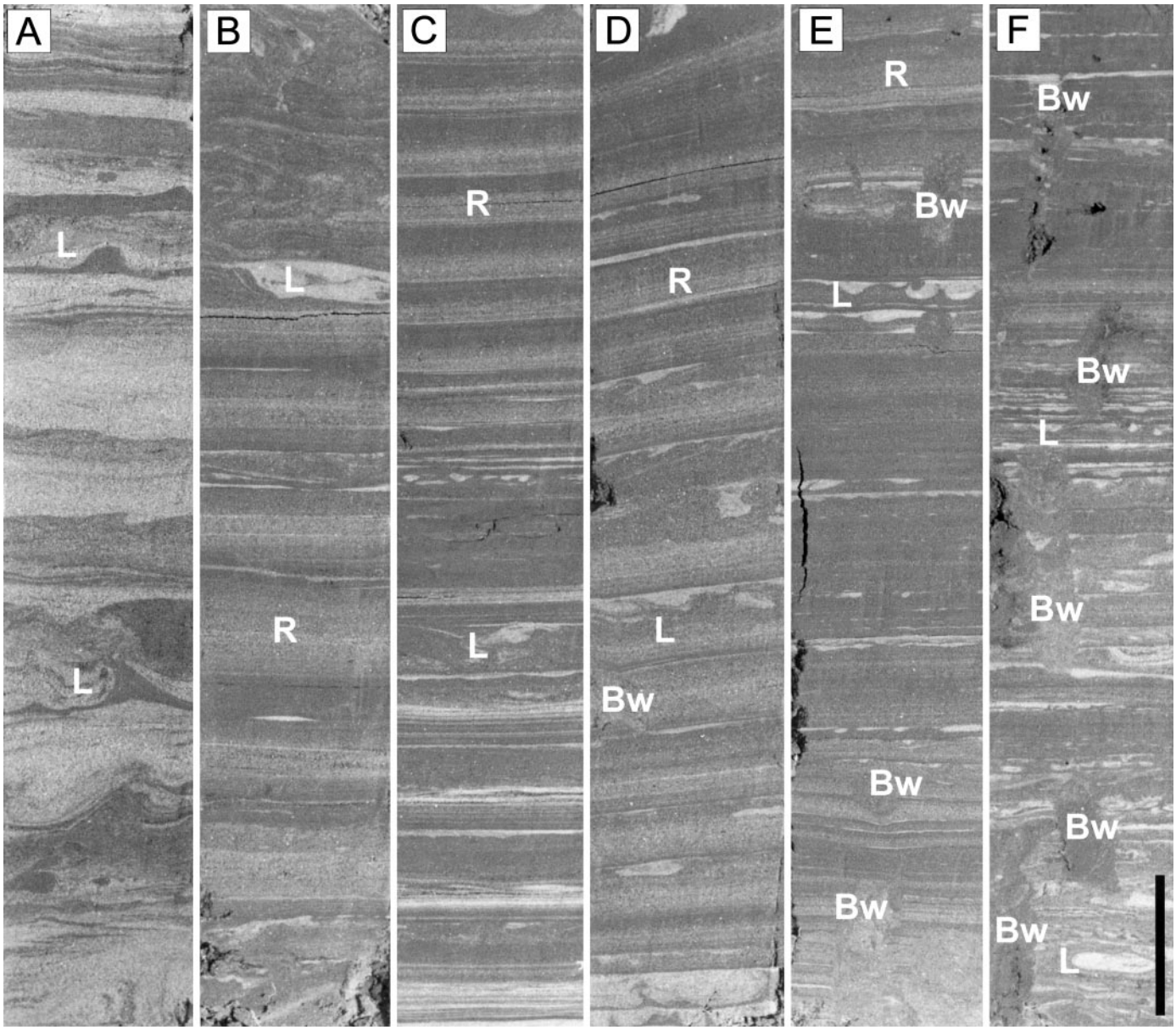

FIG. 9.—Photographs showing representative sedimentary facies: laminated sandy silt (A, B), laminated silt (C, D), and laminated mud (E, F). Light-colored material is sand; dark-colored material is mud. Refer to Figure 5 for sample locations: **A)** lower intertidal zone (−2.6 m), **B)** middle intertidal zone (−0.2 m), **C)** middle intertidal zone (+1.3 m), **D)** middle intertidal zone (+1.6 m), **E)** upper intertidal zone (+2.1 m), **F)** upper intertidal zone (+2.4 m). Burrows (Bw) become more abundant with increasing elevation, whereas load structures (L) occur at all elevations. Rapid sedimentation is indicated by the presence of tidal rhythmites (R). Note that lamina thickness and size of deformation structures generally decrease from lower (A) to higher (F) elevations. Scale bar in (F) is 3 cm.

part of the succession. Small-scale, concave-up truncation surfaces, associated with the erosional scarps, are present in the lower intertidal zone, and very large slide surfaces may cut the entire upper part of the succession. Because of the development of these truncation surfaces, the heterolithic stratification is expected to show poor continuity in the dip direction, at least in the lower intertidal portion of the succession, where wave action is concentrated. It is also probable that the subtidal portion of the succession has a poor continuity in the dip direction because of slumping. By contrast, the stratification exhibits good continuity along depositional strike.

Implications for the Interpretation of IHS

The vertical succession being created on the Sukmo Channel bank (Fig. 15) displays many features that are similar to previously described IHS, including the upward-fining grain-size trend. It differs most notably from other modern examples in its great total thickness and in the substantial thickness of cross-bedded sand in the lower part of the channel. These differences reflect the bedrock-confined, energetic setting in which this occurrence forms.

Previously reported examples of modern IHS forming in deep tidal channels were interpreted to owe their heterolithic nature to seasonal discharge variations rather than daily tidal-current action (Thomas et al. 1987; Smith 1988). Despite significant discharge variations in the Han River, the lithologic heterogeneity in the Sukmo Channel bank is almost entirely of tidal origin. However, the muddy layers do not extend to the bottom of the channel, even though the currents stop everywhere, presumably because the strong tidal currents in the deeper part of the channel erode the mud drapes.

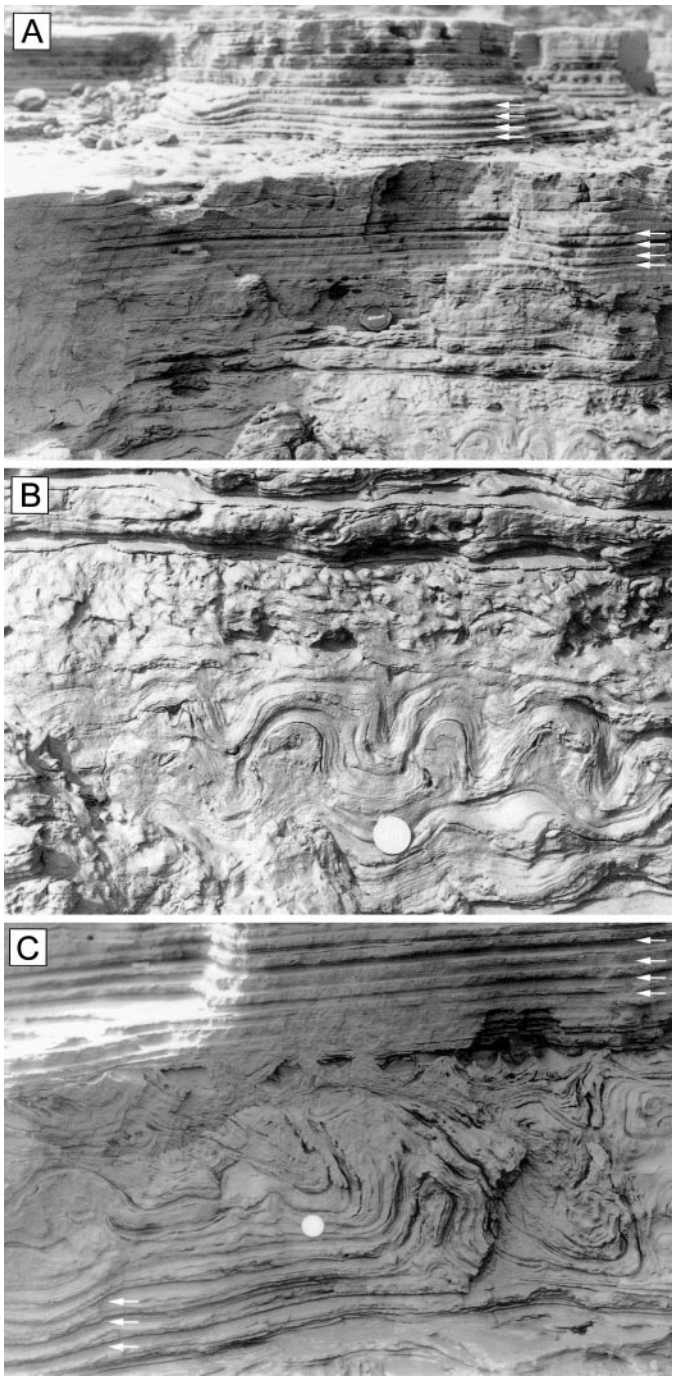

FIG. 10.—Photographs showing rhythmic lamination (A) and convolute lamination (B, C) in middle intertidal zone. Recessive laminae (arrows) in A and C represent sandier material deposited during spring tides. Diameter of lens cap (A) is 6.5 cm. Coin (B, C) is 2.5 cm diameter. Note that convolute lamination is sharply truncated by erosion surface (C). The sharply overturned anticline (C) suggests that deformation may be a result of downslope movement to the left.

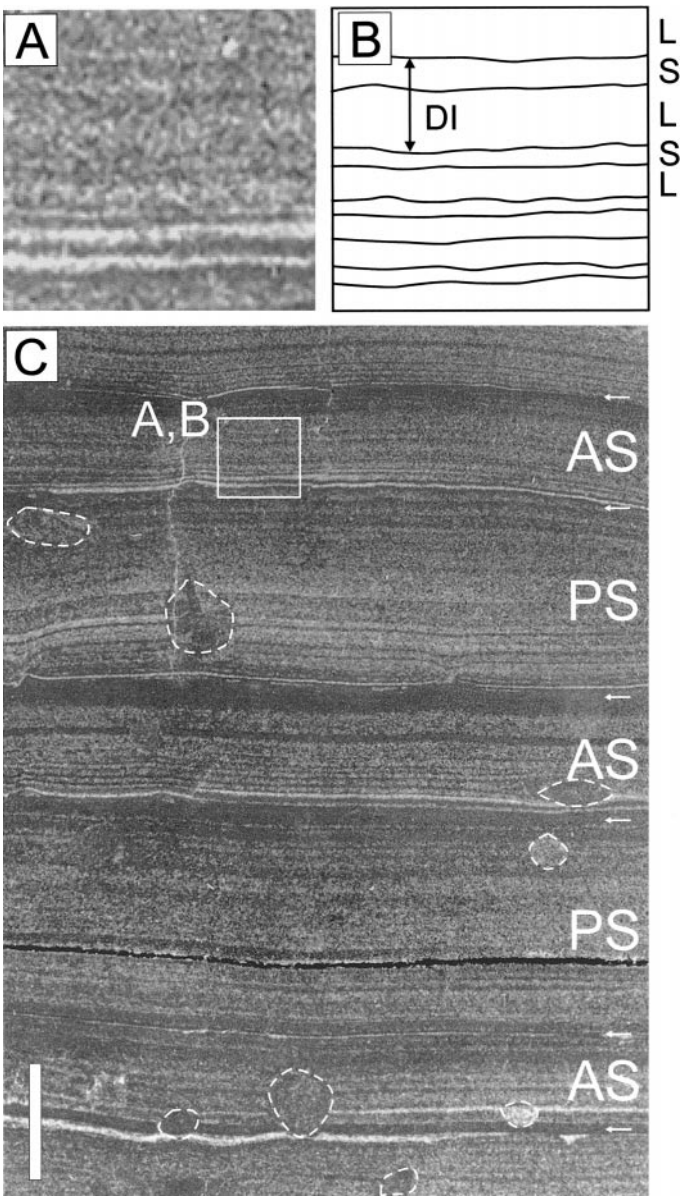

FIG. 11.—Photographs and line drawing of rhythmic tidal lamination (+0.8 m) showing hierarchical tidal cycles: (A, B) diurnal inequality (DI; L, thick lamina deposited by large tide; S, thin lamina deposited by small tide); and (C) alternation of thinner neap–spring cycles deposited during lunar apogee (AS) and thicker neap–spring cycles deposited during lunar perigee (PS). Arrows indicate inferred neap-stage laminae. Several small crab burrows (outlined by white dashed lines) are visible. Scale bar is 1 cm. See Figure 12 for lamina-thickness measurements.

Despite the nearly ideal conditions for the formation of tidal rhythmites (macrotidal environment in a protected, inshore setting with abundant suspended-sediment supply), they apparently are preserved well only above mean sea level (Fig. 15), where biological and physical disturbances are not significant; even relatively small waves (perhaps only a few centimeters high) are sufficient to disrupt the regular accumulation of sediment near the low-water level, presumably because the sediment is water saturated. This suggests that the preservation of perfect tidal rhythmites requires very sheltered conditions (i.e., in channels that are significantly narrower than Sukmo Channel).

Concave-upward erosion surfaces are a moderately common feature of IHS. In most previously described examples, these erosion surfaces have their base at the thalweg level, because they are caused either by widening of the channel to accommodate increased runoff (due to seasonal discharge variations or local rainfall), or because the channel thalweg locally cuts into the depositional bank (Bridges and Leeder 1976; De Mowbray 1983; Zaitlin 1987; Dalrymple and Zaitlin 1994). The IHS in the study area differs in that the erosion surfaces occur mainly within the lower-intertidal

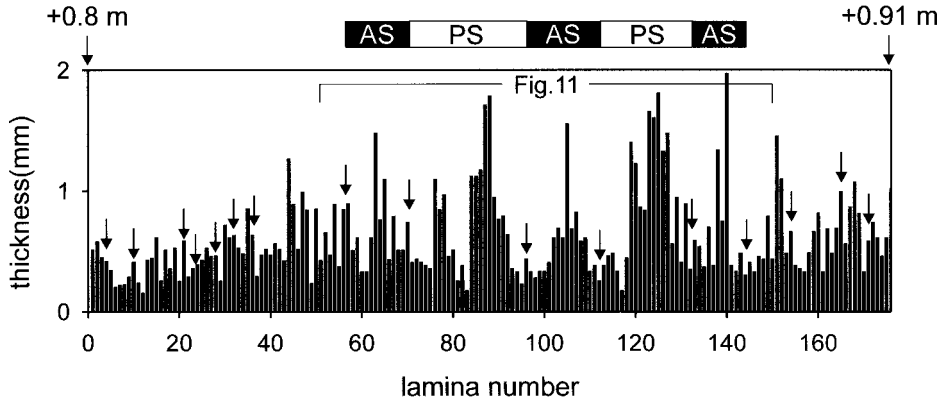

FIG. 12.—Plot of lamina thicknesses showing tidal cyclicities. Arrows indicate inferred neap-stage laminae. Elevations at top of figure are distances above mean sea level. AS and PS denote neap–spring cycles deposited during lunar apogee and lunar perigee, respectively.

portion of the succession. We attribute this difference to a combination of the following factors: the relative variability of discharge, differences in channel size, and the location of the channel within the drainage network. Channels with relatively small discharge variability are less likely to experience wholesale widening and the formation of major erosion surfaces in the point bar. In this regard, it is more difficult to produce a significant discharge increase in a large channel than in a small one, especially if the large channel is located in a distributary network (as Sukmo Channel is) because the discharge is split between several channels. By comparison, small channels near the head of tidal-creek systems are more likely to experience proportionately large discharge variations. Large channels such as Sukmo Channel are also more prone to the development of local waves than small channels and are therefore more likely to contain wave-generated erosion scours near the low-water level.

Thomas et al. (1987) discussed a range of varieties of IHS that they attributed to the relative influence of river flow and tidal currents. With increasing tidal influence in the fluvial–marine transition, for instance, the heterolithic stratification is thought to become more rhythmic in nature (e.g., Smith 1988; Rahmani 1988; Ainsworth and Walker 1994; Eberth 1996). Rhythmic IHS may also be best developed beneath the turbidity maximum because of the ability to record short-duration slack-water periods (Ainsworth and Walker 1994). However, more seaward locations

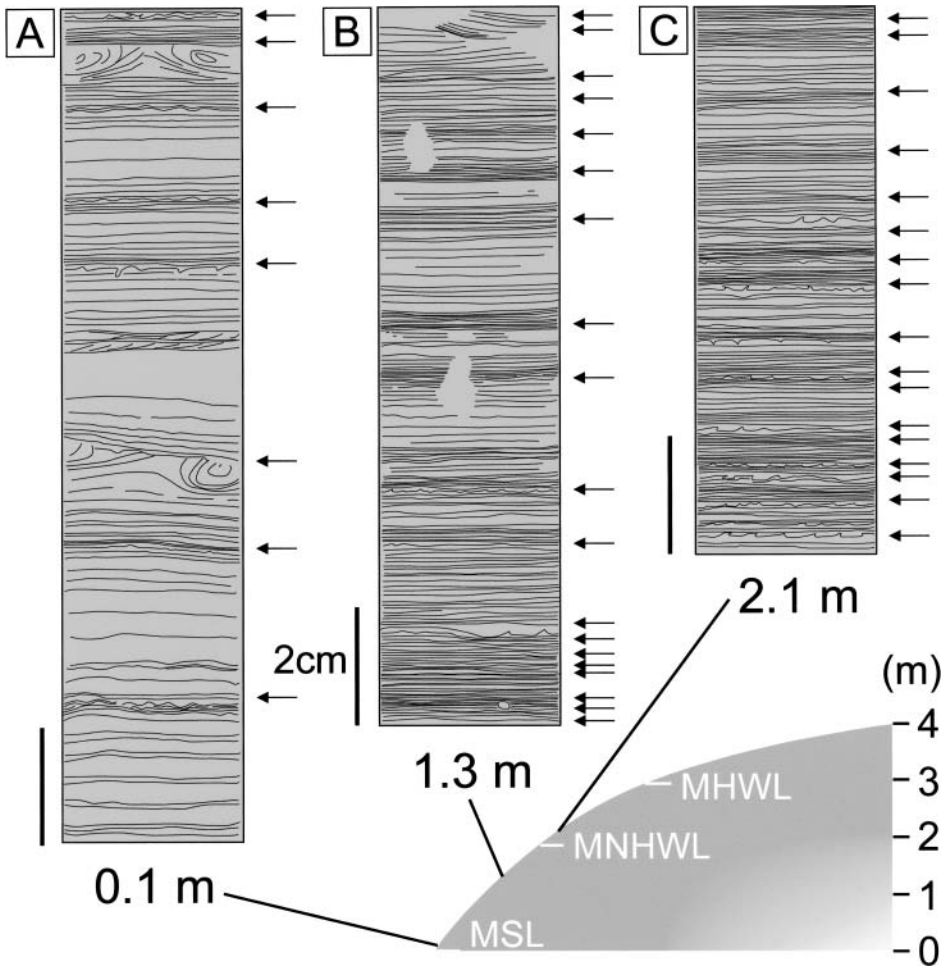

FIG. 13.—Line drawings showing variation of rhythmic tidal lamination (tidal rhythmites) with increasing elevation. Arrows indicate inferred neap-stage laminae. Thicknesses of neap–spring cycles become smaller with increasing elevation. Note that convolute lamination commonly occurs in thick, spring-tide laminae. Refer to Figure 5 for location. Vertical scale bars in A–C are 2 cm. MSL, mean sea level; MNHWL, mean neap high-water level; MHWL, mean high-water level.

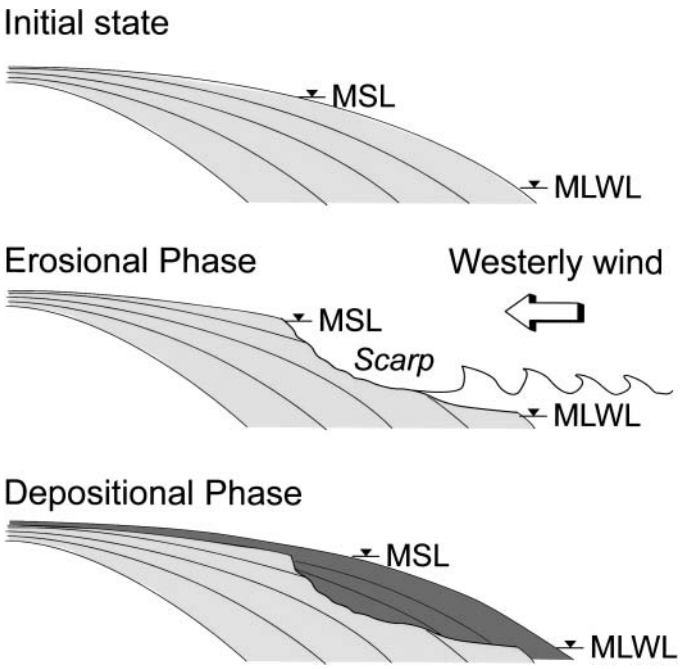

FIG. 14.—Conceptual diagrams showing temporal variation of channel-bank morphology. Note alternation of smooth convex-up shape during depositional phase and terraced morphology during erosional phase. Compare with Figure 8. Erosional scarps are mainly present below mean sea level (MSL). MLWL: mean low-water level.

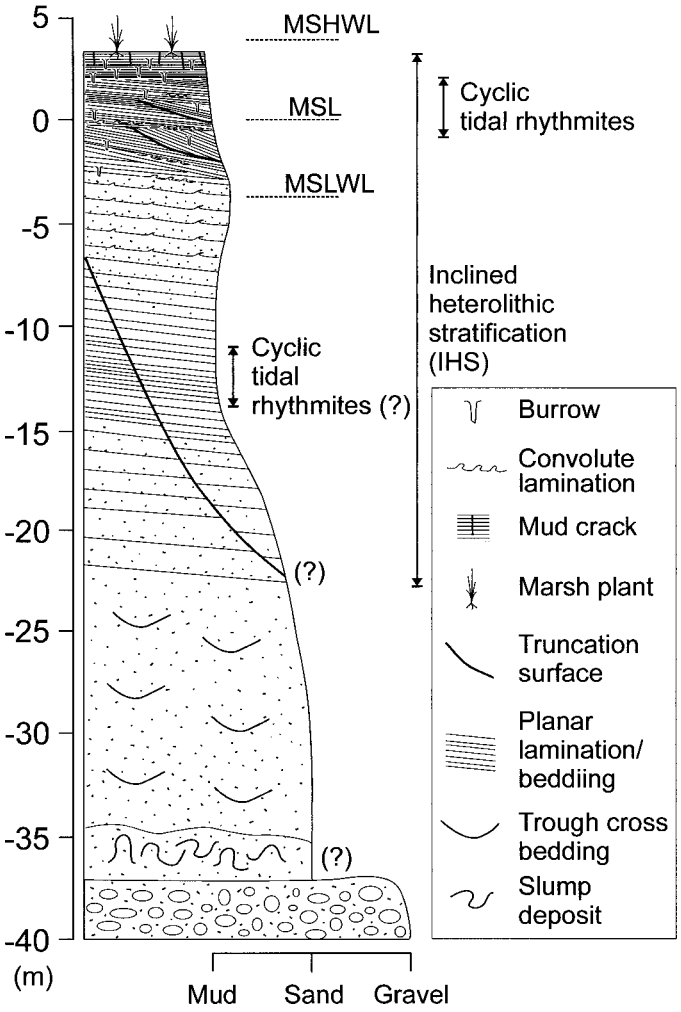

FIG. 15.—Schematic columnar section of Sukmo Channel bank near Oepori Port. Note that inclined heterolithic stratification extends through the entire intertidal and shallow subtidal portion (upper 25 m) of the bank. Tidal rhythmites are present mainly in the upper intertidal zone, and may also be present in the shallow subtidal zone. Coarsening near the MSLWL is attributed to wave influence. The cross-bedded medium sand below −25 m is flood dominated; ebb-oriented cross bedding may occur at the very base of the succession. The IHS may be cut by large-scale slump scars, with chaotic debris near the channel base. MSLWL, mean spring low-water level; MSL, mean sea level; MSHWL, mean spring high-water level.

have a higher probability of experiencing significant wave action, either because of waves arriving from the sea or because the channel is sufficiently wide that locally generated waves may be large enough to decrease the preservation potential of cyclic rhythmites as is the case in the study area.

Despite the fact that Sukmo Channel is ebb dominant, the echograms indicate that most of the cross bedding preserved within the depositional bank is likely to be flood-oriented. The reason for this counter-intuitive result is that the Oepori point bar is sheltered from the full force of the ebb currents, which are fastest on the southwestern (cutbank) side of the channel (Fig. 1B); by contrast, the flood current, following a mutually evasive path, is strongest on point-bar side of the channel. Such a situation is probably not unique to the study area; indeed, this paleocurrent pattern may be a general feature of meandering tidal systems. In such situations, we speculate that the dominant ebb flow will cause the point bar as a whole to migrate in a seaward direction, producing seaward-dipping IHS, within which the smaller cross beds dip predominantly in the flood direction.

CONCLUSIONS

Inclined heterolithic stratification (IHS) is being formed in the Sukmo distributary channel of the tide-dominated Han River delta. The IHS occupies the upper 25 m of a 40-m-thick, upward-fining channel-bank succession, the lower 15 m of which consists of medium sand that contains flood-oriented cross bedding despite the ebb-dominated nature of the channel. The IHS itself shows an upward thinning of the interbedded sand and mud layers. Tidal rhythmites are preserved in the middle and upper intertidal zone at the top of the succession and may also be present in the subtidal zone. Wave action near the low-tide level produces slightly coarser-grained deposits and prevents the formation of rhythmic lamination. Locally generated waves also produce concave-up erosion surfaces at this level. This modern example expands the range of settings in which IHS has been documented and may provide an analogue for some of the occurrences of very large IHS described from the rock record.

ACKNOWLEDGMENTS

This work was partly supported by a Korea Science & Engineering Foundation (KOSEF) postdoctoral fellowship granted to the first author (KSC). This study was also supported grants from the Natural Sciences and Engineering Research Council of Canada (#7553-01; RWD) and the Korea Science and Engineering Foundation (#R01-2001-00081; SSC). We thank M. Gingras, D. Smith, E. Kvale, M. Kraus, and J. Southard for their constructive reviews of the manuscript. We also thank Y.S. Chu (Korea Ocean Research Development Institute) for allowing us to use the echo sounder.

REFERENCES

AINSWORTH, R.B., AND WALKER, R.G., 1994, Control of estuarine valley-fill deposition by fluctuations of relative sea-level, Cretaceous Bearpaw–Horseshoe Canyon transition, Drumheller, Alberta, Canada, *in* Dalrymple, R.W., Boyd, R., and Zaitlin, B.A., eds., Incised Valley Systems: Origin and Sedimentary Sequences: SEPM, Special Publication 51, p. 159–174.

ALLEN, J.R.L., 1963, The classification of cross-stratified units, with notes on their origin: Sedimentology, v. 2, p. 93–114.

ALLEN, J.R.L., 1985, Intertidal drainage and mass-movement processes in the Severn Estuary: rills and creeks (pills): Geological Society of London, Journal, v. 142, p. 13–28.

ANIMA, R.J., CLIFTON, H.E., AND PHILLIPS, R.L., 1989, Comparison of modern and Pleistocene estuarine facies in Willapa Bay, Washington, *in* Reinson, G.E., ed., Modern and Ancient Examples of Clastic Tidal Deposits—A Core and Peel Workshop: Canadian Society of Petroleum Geologists, p. 1–19.

BARWIS, J.H., 1978, Sedimentology of some South Carolina tidal-creek point bars, and a comparison with their fluvial counterparts, *in* Miall, A.D., ed., Fluvial Sedimentology: Canadian Society of Petroleum Geologists, Memoir 5, p. 129–160.

BEETS, D.J., DE GROOT, T.A.M., AND DAVIES, H.A., 2003, Holocene tidal back-barrier development at decelerating sea-level rise: a 5 millennia record, exposed in the western Netherlands: Sedimentary Geology, v. 158, p. 117–144.

BRIDGES, P.H., AND LEEDER, M.R., 1976, Sedimentary model for intertidal mudflat channels, with examples from the Solway Firth, Scotland: Sedimentology, v. 23, p. 533–552.

CHANG, H.-D., AND OH, J.-K., 1991, Depositional sedimentary environments in the Han River estuary and around the Kyonggi Bay posterior to the Han River's developments: Oceanological Society of Korea, Journal, v. 26, p. 13–23.

CHOI, K.S., KIM, B.O., AND PARK, Y.A., 2001, Late Pleistocene tidal rhythmites in Kyunggi Bay, west coast of Korea: a comparison with simulated rhythmites based on modern tides and implications for intertidal positioning: Journal of Sedimentary Research, v. 71, p. 680–691.

CLIFTON, H.E., 1983, Discrimination between subtidal and intertidal facies in Pleistocene deposits, Willapa Bay, Washington: Journal of Sedimentary Petrology, v. 53, p. 353–369.

COTTER, E., AND DRIESE, S.G., 1998, Incised-valley fills and other evidence of sea-level fluctuations affecting deposition of the Catskill Formation (upper Devonian), Appalachian foreland basin, Pennsylvania: Journal of Sedimentary Research, v. 68, p. 347–361.

DALRYMPLE, R.W., AND ZAITLIN, B.A., 1994, High-resolution sequence stratigraphy of a complex, incised valley succession, the Cobequid Bay–Salmon River estuary, Bay of Fundy, Canada: Sedimentology, v. 41, p. 1069–1091.

DALRYMPLE, R.W., BAKER, E.K., HARRIS, P.T., AND HUGHES, M.G., 2003, Sedimentology and stratigraphy of a tide-dominated, foreland-basin delta (Fly River, Papua New Guinea), *in* Sidi, F.H., Nummedal, D., Imbert, P., Darman, H., and Posamentier, H.W., eds., Tropical Deltas of Southeast Asia—Sedimentology, Stratigraphy, and Petroleum Geology: SEPM, Special Publication 76, p. 147–173.

DALRYMPLE, R.W., MAKINO, Y., AND ZAITLIN, B.A., 1991, Temporal and spatial patterns of rhythmite deposition on mud flats in the macrotidal Cobequid Bay–Salmon River estuary, Bay of Fundy, Canada, *in* Smith, D.G., Reinson, G.E., Zaitlin, B.A., and Rahmani, R.A., eds., Clastic Tidal Sedimentology: Canadian Society of Petroleum Geologists, Memoir 16, p. 137–160.

DE MOWBRAY, T., 1983, The genesis of lateral accretion deposits in recent intertidal mudflat channels, Solway Firth, Scotland: Sedimentology, v. 30, p. 425–435.

EBERTH, D.A., 1996, Origin and significance of mud-filled incised valleys (Upper Cretaceous) in southern Alberta, Canada: Sedimentology, v. 43, p. 459–477.

FALCON-LANG, L.H., 1998, The impact of wildfire on an Early Carboniferous coastal environment, North Mayo, Ireland: Palaeogeography, Palaeoclimatology, Palaeoecology, v. 139, p. 121–138.

GINGRAS, M.K., PEMBERTON, S.G., SAUNDERS, T.D.A., AND CLIFTON, H.E., 1999, The ichnology of modern and Pleistocene brackish-water deposits at Willapa Bay, Washington: Variability in estuarine setting: Palaios, v. 14, p. 352–374.

GINGRAS, M.K., RÄSÄNEN, M., AND RANZI, M., 2002, The significance of bioturbated inclined heterolithic stratification in the southern part of the Miocene Solimoes Formation, Rio Acre, Amazonia Brazil: Palaios, v. 17, p. 591–601.

JACKSON, R.G., 1981, Sedimentology of muddy fine-grained channel deposits in meandering streams of the American middle west: Journal of Sedimentary Petrology, v. 51, p. 1169–1192.

KIER (KOREA INSTITUTE OF ENERGY AND RESOURCES), 1987, Marine investigation report for the development of coastal islands, 42 p.

KHO (KOREA HYDROGRAPHIC OFFICE), 2000, Tidal tables, v. 1: Publication no. 1201-1, 250 p.

KMA (KOREA METEOROLOGICAL ADMINISTRATION), 2001, Annual Climatological Report (year 2000): Publication no. 11-1360000-000016-10, 284 p.

KMA (KOREA METEOROLOGICAL ADMINISTRATION), 2003, Annual Climatological Report (year 2002): Publication no. 11-1360000-000016-10, 254 p.

KVALE, E.P., AND VONDRA, C.F., 1993, Effects of relative sea-level changes and local tectonics on a lower Cretaceous fluvial to transitional marine sequence, Bighorn Basin, Wyoming, U.S.A., *in* Marzo, M., and Puigdefabregas, C., eds., Alluvial Sedimentation: International Association of Sedimentologists, Special Publication 17, p. 383–399.

KVALE, E.P., FRASER, G.S., ARCHER, A.W., ZAWISTOSKI, A., KEMP, N., AND MCGOUGH, P., 1994, Evidence of seasonal precipitation in Pennsylvanian sediments of the Illinois Basin: Geology, v. 22, p. 331–334.

KVALE, E.P., JOHNSON, H.W., SONETT, C.P., ARCHER, A.W., AND ZAWISTOSKI, A., 1999, Calculating lunar retreat rates using tidal rhythmites: Journal of Sedimentary Research, v. 69, p. 1154–1168.

LARSONNEUR, C., 1994, The bay of Mont-Saint-Michel: a sedimentation model in a temperate macrotidal environment: Senckenbergiana Maritima, v. 24, p. 3–63.

LAWLER, D.M., WEST, J.R., COUPERTHWAITE, J.S., AND MITCHELL, S.B., 2001, Application of a novel automatic erosion and deposition monitoring system at a channel bank site on the tidal river Trent, U.K.: Estuarine, Coastal and Shelf Science, v. 53, p. 237–247.

MAKASKE, B., AND NAP, R.L., 1995, A transition from a braided to a meandering channel facies, showing inclined heterolithic stratification (late Weichselian, central Netherlands): Geologie en Mijnbouw, v. 74, p. 13–20.

MARTINIUS, A.W., KAAS, I., NÆSS, A., HELGESEN, G., KJÆREFJORD, J.M., AND LEITH, D.A., 2001, Sedimentology of the heterolithic and tide-dominated Tilje Formation (Early Jurassic, Halten Terrace, offshore mid-Norway), *in* Martinsen, O.J., and Dreyer, T., eds., Sedimentary Environments Offshore Norway—Paleozoic to Recent: Norwegian Petroleum Society, Special Publication 10, Amsterdam, Elsevier, p. 103–144.

MCT (MINISTRY OF CONSTRUCTION AND TRANSPORTATION), 2001, Hydrological Annual Report in Korea (year 2000): Publication no. 11-1500000-000580-10, 452 p.

MOSSOP, G.D., AND FLACH, P.D., 1983, Deep channel sedimentation in the Lower Cretaceous McMurray Formation, Athabasca Oil Sands, Alberta: Sedimentology, v. 30, p. 493–509.

PAGE, K.J., NANSON, G.C., AND FRAZIER, P.S., 2003, Floodplain formation and sediment stratigraphy resulting from oblique accretion on the Murrumbidgee River, Australia: Journal of Sedimentary Research, v. 73, p. 5–14.

PLINT, A.G., AND WADSWORTH, J.A., 2003, Sedimentology and palaeogeomorphology of four large valley systems incising delta plains, western Canada Foreland Basin: implications for mid-Cretaceous sea-level changes: Sedimentology, v. 50, p. 1147–1186.

RAHMANI, R.A., 1988, Estuarine tidal channel and nearshore sedimentation of a late Cretaceous epicontinental sea, Drumheller, Alberta, Canada, *in* de Boer, P.L., van Gelder, A., and Nio, S.D., eds., Tide-Influenced Sedimentary Environments and Facies: Dordrecht, The Netherlands, Reidel Publishing Company, p. 433–471.

REINECK, H.E., 1958, Longtidinale Schrägschichten im Watt: Geologische Rundschau, v. 47, p. 73–82.

SHANLEY, K.W., MCCABE, P.J., AND HETTINGER, R.D., 1992, Tidal influence in Cretaceous fluvial strata from Utah, U.S.A.: A key to sequence stratigraphic interpretation: Sedimentology, v. 39, p. 905–930.

SHANMUGAM, G., POFFENBERGER, M., AND ALAVA, J.T., 2000, Tide-dominated estuarine facies in the Hollin and Napo ('T' and 'U') formations (Cretaceous), Sacha field, Oriente basin, Ecuador: American Association of Petroleum Geologists, Bulletin, v. 84, p. 652–682.

SMITH, D.G., 1987, Meandering river point bar lithofacies models: modern and ancient examples compared, *in* Ethridge, F.G., Flores, R.M., and Harvey, M.D., eds., Recent Developments in Fluvial Sedimentology: SEPM, Special Publication 39, p. 83–91.

SMITH, D.G., 1988, Modern point bar deposits analogous to the Athabasca Oil Sands, Alberta, Canada, *in* de Boer, P.L., van Gelder, A., and Nio, S.D., eds., Tide-Influenced Sedimentary Environments and Facies: Dordrecht, The Netherlands, Reidel Publishing Company, p. 417–432.

STANLEY, K.O., AND SURDAM, R.C., 1978, Sedimentation on the front of Eocene Gilbert-type deltas, Washakie Basin, Wyoming: Journal of Sedimentary Petrology, v. 48, p. 557–573.

TESSIER, B., 1993, Upper intertidal rhythmites in the Mont-Saint-Michel Bay (NW France): perspectives for paleoreconstruction: Marine Geology, v. 110, p. 355–367.

THOMAS, R.G., SMITH, D.G., WOOD, J.M., VISSER, J., CALVERLEY-RANGE, E.A., AND KOSTER, E.H., 1987, Inclined heterolithic stratification—terminology, description, interpretation and significance: Sedimentary Geology, v. 53, p. 123–179.

ZAITLIN, B.A., 1987, Sedimentology of the Cobequid Bay–Salmon River Estuary, Bay of Fundy, Canada [unpublished Ph.D. thesis]: Queen's University, Kingston, Ontario, Canada, 391 p.

Received 4 August 2003; accepted 8 March 2004.